Earth Science Informatics
https://doi.org/10.1007/s12145-023-01001-y

RESEARCH

A 3D geological model of the Gallocanta Basin (Spain). The basis to update the hydrogeological model

Javier Ramajo[1] · Jose María Orellana-Macías[2] · Carlos Galé[3] · Manuel Arce[4] · Jesús Causapé[1]

Received: 12 December 2022 / Accepted: 14 March 2023

Abstract

Three-dimension geological models represent the subsurface geology based on the development of 3D geological structures as an extension of geological maps. This study aims to update the previous geological information of the Gallocanta Basin (NE Spain) by (1) extending the model domain to most parts of the basin and (2) developing a new 3D model. The ultimate objective is to obtain a 3D geological model which provides a more detailed conceptual understanding of the groundwater flow for a future hydrogeological model. We used MOVE 2017 software to render the geological data and develop the new model. The geological 3D model has shown the effectiveness of using three-dimensional analysis as a useful tool for the geological reconstruction of complex areas. The creation of the present three-dimensional model constitutes the basis for geological and hydrogeological works.

Keywords Geological map · 3D geological modelling · Hydrogeological unit · Gallocanta

Introduction

Three-dimension models show the subsurface geology through the construction of 3D geological structures as an extension of geological maps (Wellmann et al. 2019). In the last decades, three-dimension geological mapping and modelling (*geomodeling*) have been rapidly developed as a tool for precisely defining the subsurface conditions (Turner and Gable 2007). This development has been facilitated by improvements in technology and software (Berg and Thorleifson 2001). Three-dimension models are used to solve uncertainties related to human-environmental issues and economic interests (Haldar 2018), and they have proven to be useful to several disciplines such as the study of gas and petrol reservoirs (Zhuang 2013), the exploration of structural geology and tectonics (Thornton et al. 2018), the creation of earthquake location catalogues (Béthoux et al. 2016), or the sustainable use of groundwater and its protection (Berg and Thorleifson 2001; Artimo et al. 2003; Turk et al. 2015). Recently, they have also contributed to facing current environmental and engineering issues such as radioactive waste storage (Mont Terri Project 2017) or engineering projects (Vanneschi et al. 2014).

Concerning groundwater management, the use of geomodeling have been widely used as an input for numerical groundwater modelling (Jørgensen et al. 2015) to estimate groundwater resources (Hassen et al. 2016) and enhance its sustainability and protection (Ross et al. 2005; Howahr 2016), as well as for simulating groundwater flows and directions (Malard et al. 2015; Ballesteros et al. 2015), and provide data for modelling in relation to geothermal energy facilities (Guglielmetti et al. 2013; Zhu et al. 2020).

Kessler et al. (2007) pointed out that a robust geological model helps to understand the hydrogeological framework of an area, and it is an essential basis to develop a reliable hydrogeological model.Also, Robins et al. (2005) noted that the geological framework and conceptual groundwater model should be analysed together to prevent misunderstanding of the relation between the geological structure and the hydrogeology. The over-simplification of geological structures in groundwater models can lead to unrealistic

Communicated by: H. Babaie.

✉ Jose María Orellana-Macías
jmariaorellana@gmail.com

[1] Centro Nacional Instituto Geológico y Minero de España-CN-IGME, CSIC. Av. Montañana 1005, 50059 Zaragoza, Spain

[2] Vitoria-Gasteiz, Spain

[3] IDEYA Red Profesional, Av. De la Autonomía 7, 50003 Zaragoza, Spain

[4] H2i Analytics, Zaragoza, Spain

results and unreliable modelling outputs (Kessler et al. 2007), so the more accurate the geological description used as input, the more consistent results. The detailed geologic characterization not only consists of describing geological structures, thrusts and folds but also must include the distribution, thickness, extension, stratigraphy and sedimentology of the rocks (Artimo et al. 2003). The geologic characterization aims to provide a detailed picture of the sub-surface geology and a reliable geological conceptual model, which could be used both by researchers and planners.

The geological setting of the Gallocanta Basin has been studied in the last decades. Villena (1969) elaborated the first geological map of the area, and the Geological Survey of Spain (IGME from its Spanish acronym) mapped the geology of the area within the MAGNA Project (Bascones and Martín, 1979; Del Olmo and Portero 1980; Hernández et al. 1980a, 1980b; Olivé et al. 1980; Portero et al. 1980)

During the following years, the geological studies focused on geomorphology and sedimentology aspects (Gracia 1990a, 1990b, 1992, 1995; Schütt 1998, Luzón et al. 1999; Pérez et al. 1999). These works followed the geological interpretation proposed by Hernández Pacheco and Aranguren (1926) and Dantín (1941), which considered the Gallocanta depression as a *graben* developed by the activity of a fault located in the north-eastern boundary of the basin. This interpretation was refuted by Gracia et al. (1999), who proved that the basin was a structurally controlled karst large polje developed due to the dissolution of carbonate rocks during the Upper Pleistocene. The vertical dissolution ceased when it reached the impermeable Triassic substratum beneath the carbonated rocks and then started to extend horizontally (Gracia et al. 1999), which enhanced the development of water bodies like the Gallocanta Lake. The lake was formed about 12,200 yr BP, in the Late Pleistocene (Burjachs et al. 1996), and its evolution has been analysed through the study of the lake sediments and the morphology of the surrounding area (Schütt 2000; Pérez et al. 2002; Mayayo et al. 2003, Luzón et al. 2007, Castañeda et al. 2015).

In 2003, the Ebro Hydrographic Confederation (CHE from its Spanish acronym) published a detailed geological description of the area. That study compiled all the geological, hydrogeological, and geomorphological available data, as well as additional environmental data, and created the first hydrogeological model of the groundwater basin. In that work, a new geologic map was developed, and eight geological cross-sections, perpendicular to the Iberian Range orientation (NW-SE) and covering the central area of the basin, were created.

Despite some gaps and structural uncertainties, it can be considered the most exhaustive study of the area from a geological and hydrogeological perspective. However, after almost twenty years, many things could be updated. Thus, this study aimed to improve the previous model by (1) reviewing and extending the model to almost the whole Gallocanta Basin and (2) developing a new 3D model using specific software. Finally, the ultimate objective is to provide a detailed geological model to enable the development of a more accurate conceptual understanding of the local groundwater flow and, subsequently, an appropriate groundwater model.

Geology of the study area

The study area covers the Gallocanta Basin. It is a 540 km^2 endorheic catchment located in northeast Spain. The basin is within the Iberian Range, and its elevation ranges between 990 m and 1400 m in the NE (Sierra de Santa Cruz) and SW (Sierra Menera) boundaries (Fig. 1). The area is mostly flat, which enhances the development of ephemeral water bodies where the underlying rocks are impervious. The biggest water body within the basin is the Gallocanta Lake, located at the lowest part (990 m). The Gallocanta Lake is the largest saline lake in Western Europe (14.5 km^2), and it is included in the Ramsar list (Ramsar Convention Secretariat, 2010).

The study area is located at the northern margin of the Castilian branch of the Iberian Range, an intraplate mountain chain resulting from the convergence of the Eurasian and the African plate (Alvaro et al. 1979; Capote et al. 2002; De Vicente 2004).

Late-Variscan NW-SE and NE-SW striking faults played a key role in the structure of the Iberian Range (Arthaud and Matte 1975). Their reactivation as normal faults enhance the development of thick sedimentary basins during the Mesozoic rifting. The Cenozoic compression produced the inversion of the Mesozoic sedimentary basins and generated thrusts and faults with a main NW-SE direction (Capote et al. 2002; De Vicente 2004; Guimerà, 2018).

A dominant ridge in the NE part roughly divides the area into two parts: a tectonic relief that comprises the Variscan basement and an adjacent depression including the Mesozoic-Cenozoic cover and the Holocene deposits of the Gallocanta Lake (Fig. 2). The Variscan basement is characterised by NW-SE trending folds, schistosity, and low-grade metamorphism (Bauluz et al. 1998). The Mesozoic-Cenozoic cover includes a series of anticline and syncline folds and several inverse faults parallel to the main Paleozoic anticline (Fig. 2). Karstic collapses associated with the Upper Triassic sediments are also identified.

The area is dominated by deep inverse faults affecting the Mesozoic-Cenozoic cover (Fig. 2). These faults dip to the SW in the north-eastern part of the area. The layers were displaced in the NW direction as a result of a NNE to NE shortening episode during the Cenozoic compression (Liesa et al. 2018), creating inverse faults and folds striking NW-SE (Fig. 2). Towards the centre and the south of the depression, these faults tend to be more vertical concerning the diapiric movements of the Triassic sediments (Fig. 2). Dip angles in folds are usually low, except those situated

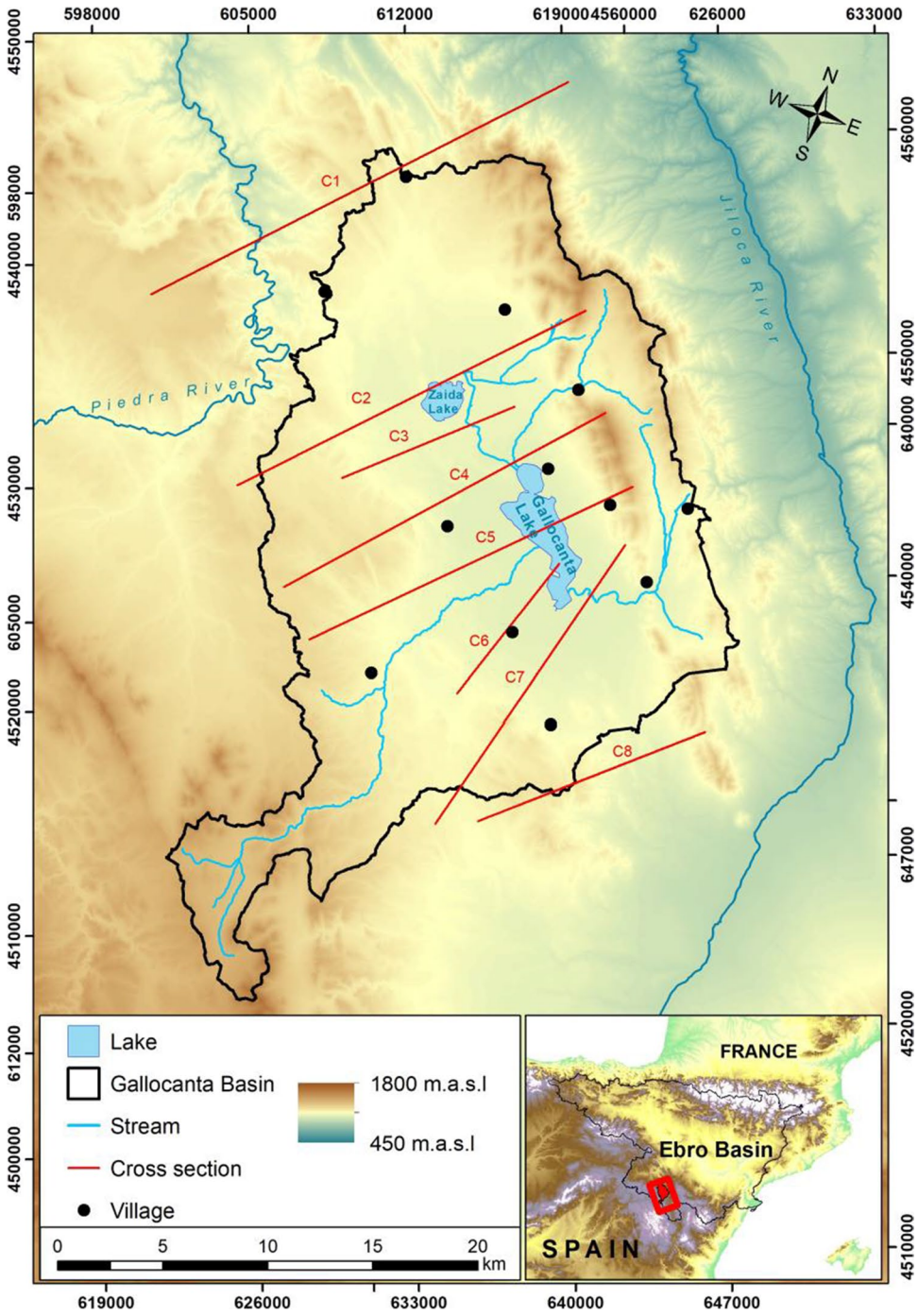

Fig. 1 Location of the study area and distribution of cross-sections

next to faults. Finally, Cenozoic materials overlay the Mesozoic deposits in the western part of the study area (Fig. 2).

Lithostratigraphy

The geological record of the area ranges from the Paleozoic to the Holocene, mostly NW-SE oriented. We distinguish eight cartographic units:

The Paleozoic is equivalent to the West Asturian-Leonese unit of the Hesperian Massif (Pérez *et al.*, 2004), and it is similar to the Badules unit defined by Lotze (1929) and Carls (1983). It ranges from Middle Cambrian to Lower-Middle Ordovician and includes different formations considered as a single unit for this work. It comprises quartzites and slates, alternated with siltstones and sandstones. The upper part of the Paleozoic (Borrachón Fm, Tremadoc age) is made up

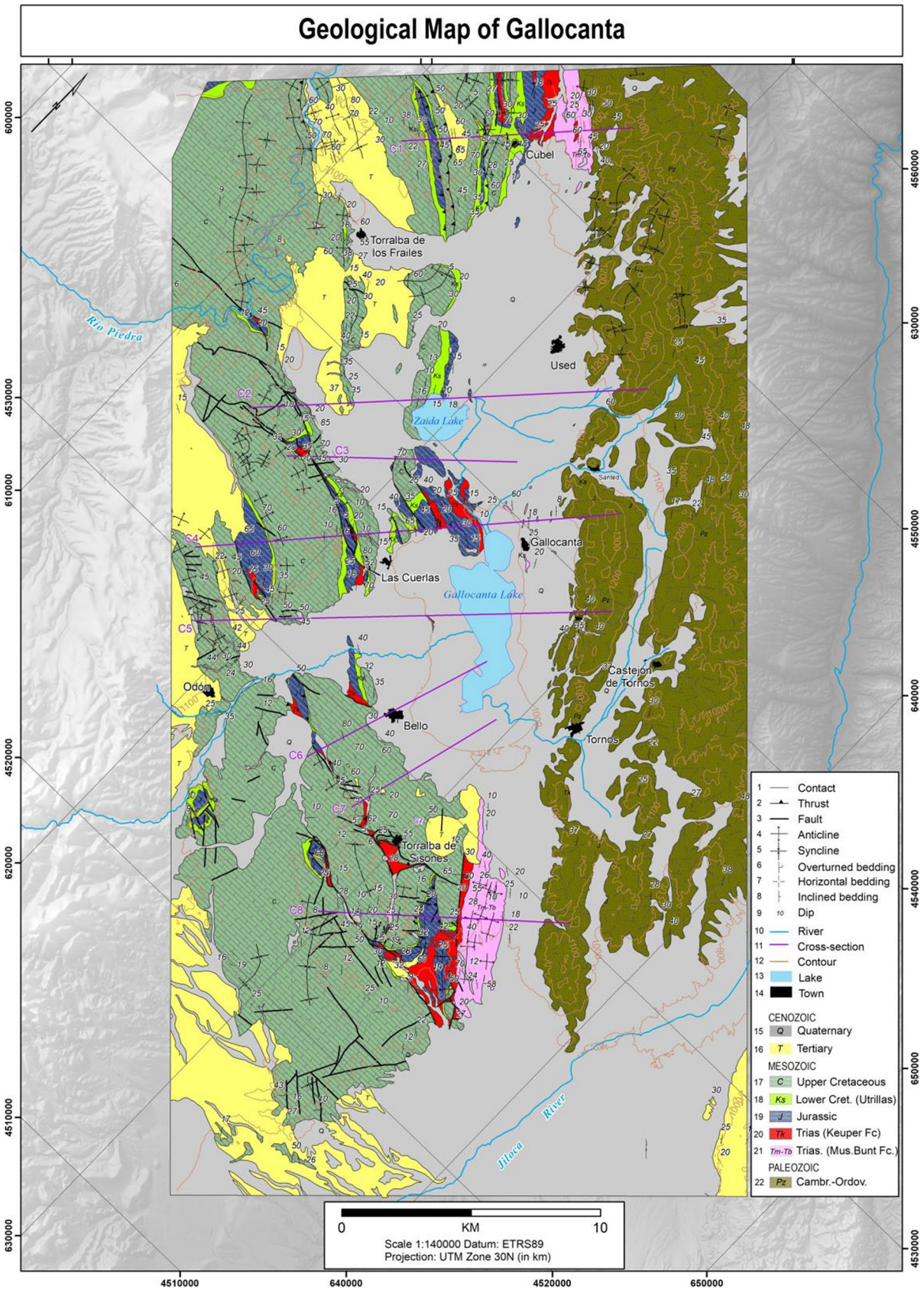

Fig. 2 Geological map of the study area

of slate and grey siltstones, alternating with thin levels of sandstones with lenticular stratification.

The Triassic record starts with the Buntsandstein unit (Lower Triassic). It is attached to the Paleozoic, at the foot of the Sierra de Pardos-Sierra de Santa Cruz (NE of the study area). Its largest outcrops are located to the north of Gallocanta Lake, below the Quaternary deposits near the lake. This unit comprises quartzite conglomerates, sandstones, versicolour shales, and, occasionally, gypsum from the Röt facies (Ramos 1979). Muschelkalk (Middle Triassic) includes dolomites alternated with dolomitic marls and recrystallised dolomites in massive banks on the top (Virgili et al. 1977). Close to the top, changes to an alternative series of tablet dolomites and micritic limestone with marls. Muschelkalk outcrops between the Paleozoic rocks and the Quaternary deposits. The Buntsandstein and Muschelkalk outcrops have been gathered within the same cartographic unit.

The Keuper unit (Upper Triassic) comprises clays and evaporites, usually intensely folded, increased in thickness, or even absent due to its plastic behaviour. This unit also plays a key role in the geology of the area, acting as a detachment level for the overlying structures or reverse fault structures.

The Jurassic is exposed in anticlinal structures of the middle-western part of the study area. It mainly consists of dolomitic breccias and vacuolar dolomites and is probably Rhaetian in age (Goy et al. 1976). There are also small patches of calcarenites and bioclastic limestones with some levels of marls of the Sinemurian- Pliensbachian age.

The Utrillas facies (Aguilar et al. 1971) overlays the Jurassic, and occasionally the Triassic, in the flanks of the anticlinal structures where the Jurassic outcrops. It is also present at the bottom of slopes, under cliffs or outcrops of the overlying Cretaceous units. It includes conglomerate, sands, and clays. This unit is Albian to Cenomanian in age. Given its soft nature, it is a level that may show non-original, sedimentary thickness variations.

The Upper Cretaceous materials correspond to the southern foothills of the Aragonese branch of the Iberian Range and consist of a series of carbonate platforms. They show intense karstification and have the highest permeability of the area. The lower part of this unit includes marls, limestones, and massive dolomitic levels (García et al. 1989; Vilas et al. 1982) and ranges between Cenomanian and Turonian in age. The upper part is mainly composed of dolomites and limestones with some marls insertions. This part is Turonian to Campanian in age.

The Cenozoic outcrops as isolated patches partially covering the Mesozoic structures. It separates into two groups based on their lithological and tectonic characteristics. The older is made up of clays, calcareous conglomerate levels, and sands and is Paleogene in age. The younger is Miocene and includes unconsolidated clays and quartzite pebbles. Finally, the Quaternary (Holocene) is mainly composed of detrital series and represents the deposit of the lake (Luzón et al. 2007).

Hydrogeology

The Borrachón Fm. (Tremadoc) comprises slates and siltstones and is considered impervious. Nevertheless, the fractures ease water transmission, so springs and small wells connected to local aquifers in quartzites proliferate in the area.

Adjacent to the Paleozoic rocks, Triassic carbonates and detrital sediments form small aquifers located in the northeast rim of the basin. They channel water from Paleozoic rocks to the lake. The Keuper unit is the impermeable basis of the upper aquifers. At some locations, it tends to form anticlinal and diapiric structures that will condition the flow directions of the aquifers.

Regarding the Mesozoic units, the Jurassic is the main carbonated aquifer of the area, with high permeability due to fracturing and karstification. Above, the Utrillas facies includes clay and act as a partially impervious layer. It works as a low hydraulic-conductivity unit, hindering the flow between its upper and lower parts (Upper Cretaceous and Jurassic, respectively). Regarding Upper Cretaceous, the marl levels of this unit are intensely fractured, and all the formations suffered strong karstification, making them behave as a single aquifer.

The Tertiary unit is essentially impermeable, although the conglomeratic and sandy facies act as an aquitard and form a small local aquifer. Finally the Quaternary deposits constitute an aquifer unit directly related to the Gallocanta Lake.

The hydrogeological parameters of the units are shown in Table 1. Those parameters have been obtained from CHE (2003). However, hydraulic conductivity has been calibrated to improve the simulation, and parameters of the Quaternary, Upper Cretaceous and Jurassic units have been modified in order to better simulate reality. In all the cases, hydraulic conductivity was reduced.

Material and methods

Materials

The geological model of this study is based on a previous model created by CHE (2003) and on the MAGNA geological cartography published by IGME. As part of the works related to the development of this model, a 1:12,500 scale

Table 1 Hydrogeological parameters of the cartographic units. Adapted from CHE (2003)

Cartographic Unit	Hydraulic conductivity (m/d)		Specific Storage	
	KX-KY	KZ	SS	SY
Quaternary	20	0.5	0.25	0.6
Tertiary	0.01	0.00005	0.0001	0.001
Upper Cretaceous	1	0.1	0.005	0.005
Lower Cretaceous (Utrillas)	0.02	0.0001	0.0001	0.001
Jurassic	5	0.5	0.00005	0.015
Keuper	0.0001	0.0001	0.0000001	0.001
Lower-Middle Triassic	1	0.005	0.00005	0.005
Paleozoic	0	0	0	0

geological map (displayed on a smaller scale for easing presentation) was created integrating fieldwork, the MAGNA geological maps (Bascones and Martín, 1979; Portero et al. 1980; Olivé et al. 1980, Hernández et al., 1983a and b, Del Olmo & Portero, 1983), the GEODE maps (López Olmedo et al. 2021), and the 1:25,000 scale geological cartography developed for the hydrogeological model by CHE (2003). Additionally, the discrepancies detected between all these maps have been verified and corrected based on fieldwork. The maps have been digitised and georeferenced by using GIS. The information about the geological structure (folds, faults), and boreholes from the official inventory of CHE (www.chebro.es), have also been included to complement the geological data.

The geological data have been divided into eight cartographic units, characterised by their lithological similarities and hydrogeological parameters to synthesise and simplify the information.

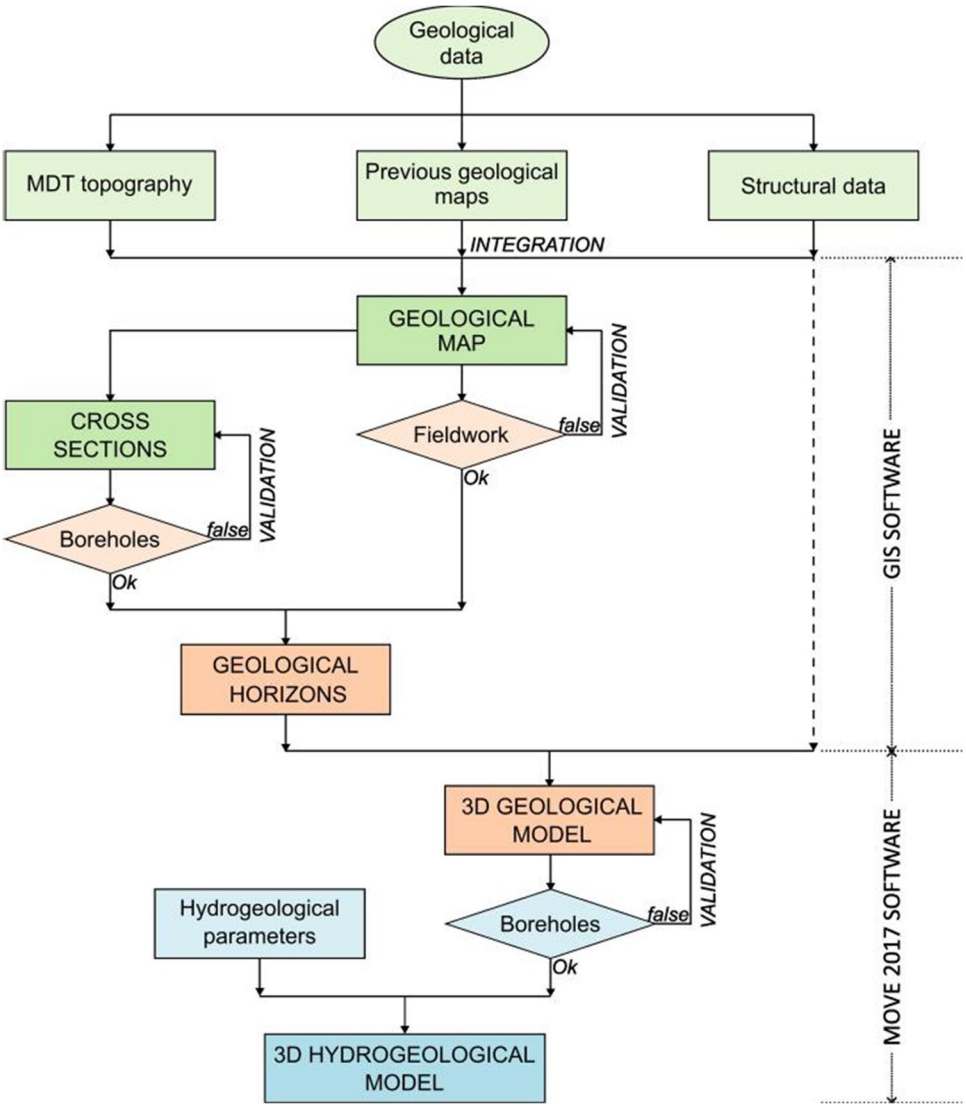

Fig. 3 Workflow followed to develop the geological model

Table 2 Cartographic Units of the model

Era	System	Series	*Cartographic Unit*	Stratigraphic Unit	Lithology	Thickness (m)
Cenozoic	Quaternary	Holocene	*Quaternary*	Lake deposits	Clay, marl and limestone	10
		Upper Pleistocene		Alluvial deposits	Sandstone, siltstone and clay	
		Middle Pleistocene		Alluvial fans	Conglomerate and sandstone	
		Lower Pleistocene		Undifferentiated Quaternary	Breccias, gravel and silt deposits	
	Neogene		*Tertiary*	Distal alluvial fans	Clay and sandstone	90
	Paleogene			Alluvial Fans	Conglomerate and sandstone	
Mesozoic	Cretaceous	Upper	*Upper Cretaceous*	Pantano de la Tranquera / Ciudad Encantada Fm.	Dolomitic breccias	600
					Karstic limestone and dolomite	
				Margas de Casa Medina Fm.	Marl and limestone	
				Villa de Ves / Alatoz Fm.	Dolomite	
				Sot de Chera Fm.	Marl	
		Lower	*Lower Cretaceous (Utrillas)*	Arenas de Utrillas Fc.	Sand and clay	90
	Jurassic	Lower	*Jurassic*	Cuevas Labradas Fm.	Limestone	200
				Cortes de Tajuña Fm.	Carbonate breccias and dolomite	
				Dolomía de Imón Fc.	Limestone and dolomite	
	Triassic	Upper	*Keuper*	Keuper Fc.	Clay and gypsum	~250
		Middle	*Lower-Middle Triassic*	Muschelkalk Fc.	Dolomite and marl	~200
		Lower		Buntsandstein Fc.	Sandstone and siltstone	~200
Paleozoic	Ordovicic	Lower-Middle	*Paleozoic*	Borrachón Fm.	Quarzitic sandstone	-

Development of the geological model

Figure 3 summarizes the workflow followed to develop the geological model. The starting point in the development of the model was the reviewed and updated geological map. This map was loaded in MOVE 2017 as polygons and lines in shapefile format, consisting of geological units and contacts. The map was clipped and fitted to cover the whole extension of the Gallocanta Basin (Fig. 2).

As aforementioned, several cartographic units were drawn: Quaternary, Tertiary, Upper Cretaceous, Lower Cretaceous (Utrillas), Jurassic, Keuper, Muschelkalk, Buntsandstein and Paleozoic. The characteristics of each unit are listed and described in Table 2. The thickness of the horizons, which represent the cartographic units, was based on field observations, data from the geological cross-sections, the previous model and boreholes. Finally, the topographic profile of the area was loaded in MOVE using a Digital Elevation Model (DEM) at 1:50.000 scale, available at the Spanish National Geographic Institute (www.ign.es).

Concerning the geological cross-sections, those obtained from the previous model have been re-assessed (C1 to C8, Fig. 1). Their extension has been extended to cover the entire basin. They have been adjusted to the new topography obtained from the DEM. The boreholes were projected into the closest cross-sections and used to calibrate the thickness of the cartographic units. In addition, the structures of the diapirs were reinterpreted based on fieldwork and knowledge of regional geology. The information has been rendered and analysed using the MOVE 2017 geological toolkit (PETEX 2017). MOVE has been also used for developing and mapping the baselines or horizons of the hydrogeological units, which have been subsequently integrated into the hydrogeological model.

Once the units were created, the eight SW-NE geological cross-sections were digitised and included in the 3D model (Fig 4). To do so, the cross-sections created for the previous model were extended to match the dimensions of our model. Then, faults, thrusts and horizons lines from cross-sections were traced and those from the geological map were also projected. *Extend* tool in MOVE was used to extend those faults affecting several units and limit the extent of those affecting only the Mesozoic rocks. The boundaries of the diapiric structures that affect the Triassic sediments were adjusted to the

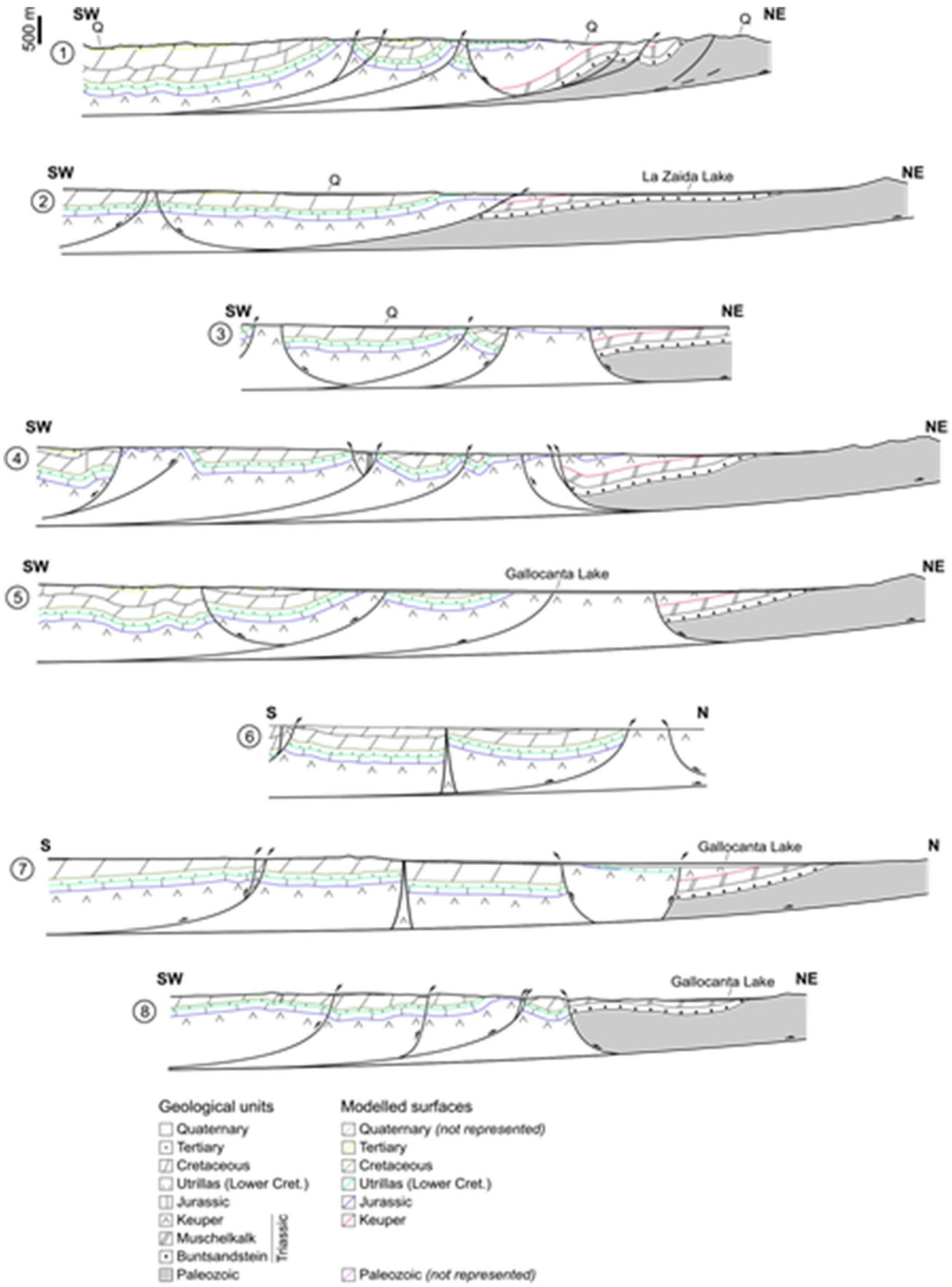
500 m
SW
NE
1
2
La Zaida Lake
3
4
5
Gallocanta Lake
S
N
6
7
8
Geological units
Quaternary
Tertiary
Cretaceous
Utrillas (Lower Cret.)
Jurassic
Keuper
Muschelkalk
Buntsandstein
Triassic
Paleozoic
Modelled surfaces
Quaternary (not represented)
Tertiary
Cretaceous
Utrillas (Lower Cret.)
Jurassic
Keuper
Paleozoic (not represented)

◂**Fig. 4** Geological cross sections used to create the geological model (locations indicated in Fig. 1). Each colour indicates the corresponding surface in the geological model (Quaternary and Paleozoic surfaces are not shown in order to ease visual understanding of the figure)

limits of the adjacent geological units according to the geological map.

Finally, the depth of the boundaries between units was compared with the data obtained from the boreholes to confirm the reliability of the 3D model. The model fit with the borehole data was good for all units except for the boundary between the Lower Cretaceous (Utrillas) and the Upper Cretaceous. The modelled boundary is located at a greater depth than in the boreholes. This is because the software considers the units to be uniform in thickness, and the Lower Cretaceous shows local variations in thickness due to its sedimentology.

Results

The main results are both the geological map and the 3D geological model. Following the previous geological works. We distinguished eight different geological units based on their hydrogeological properties (Fig. 5).

The oldest modelled unit is the Variscan Basement. It comprises the top of the Paleozoic, inferred from cross-sections, boreholes and geological maps. It also includes the Lower and Middle Triassic sediments (Buntsandstein and Muschelkalk units). According to previous works, these Triassic units do not exceed 200 m of thickness, and their hydrogeological role in the model is limited. The carbonated rocks form small aquifers in the eastern part of the lake, enhancing infill flows from the mountains through the Quaternary deposits and transferring groundwater to the north and south of the Gallocanta Groundwater Body.

The Keuper unit spans most of the study areas. This unit outcrops related to diapiric structures and determine groundwater flow from the Mesozoic aquifers. The Keuper unit is observed at shallower depths at the eastern part and acts as an impervious barrier to groundwater outflows below the Gallocanta Lake. When it is not affected by tectonics, it reaches 250 m. From a modelling perspective, this unit has been considered the basal level of the hydrogeological model, given its hydrodynamics characteristics.

The Jurassic unit overlaps the Keuper below. Its geometry is defined by the NW-SE folds, and several inverse faults determine the thickness of the sedimentary pile. The presence of diapiric structures ascending towards the surface establishes the areal extension of this unit. The shallowest depths of this unit are located around La Zaida Lake, being responsible for the groundwater contributions to this endorheic lake. The thickness of this unit does not exceed 200 m., and its geometry defines the base of the main aquifer of the study area.

The Lower Cretaceous (Utrillas) unit is a discordant unit over the Jurassic, and its thickness ranges between 60-90 m. Its characteristics determine that this unit is neither parallel to the Jurassic below nor the Upper cretaceous above. As well as the Jurassic, this unit is also affected by diapiric structures. In the 3D model, this unit has an irregular lower horizon and is interpreted as a lower permeability level due to its lithological heterogeneity (sands. conglomerates. and clays).

The Upper Cretaceous unit is the basis of the Upper Cretaceous aquifer and outcrops in the western and south-eastern parts of the study area. In western outcrops the Piedra River basin drains the aquifer. In the surroundings of the Gallocanta Lake, this unit shows a smoothly eastwards inclination draining into the Jiloca River. The maximum thickness of this unit exceeds 600 m., being the thickest unit. This unit comprises the second main aquifer in the area.

The Cenozoic unit overlays the Upper Cretaceous and outcrops in the north-eastern and south-western parts of the study area. Its extension is limited to the margins of the model area and has an average thickness of 100 m. Its connection with the Quaternary deposits is not common, suggesting that deep Cenozoic lithologies are isolated and restricted to riverbeds and lakes.

The Quaternary unit is extended across the southern and central part of the study area, comprising lacustrine Pleistocene deposits. In the northern and eastern parts, the sediments correspond to alluvial fans and glacis related to the Paleozoic relief. This unit reaches greater depths towards the south of the Gallocanta Lake. The eastern margin of the study area also has greater depths around Gallocanta Lake, whereas the thickness of the Quaternary increases towards the east and the Jiloca River. The thickness of this unit is up to 30 m in the surroundings of the lake, and its arrangement around the lake determines that this unit has a strong influence on the characteristics and behaviour of the hydrogeological model.

Discussion

Updating the geological model

The geological model presented in the first part of this research updates the cartography provided in previous works. The maps developed in this work increase the level of detail and they correct some inaccuracies of the previous maps. Likewise, the new model expands the modelled area and covers almost the entire hydrographic basin of

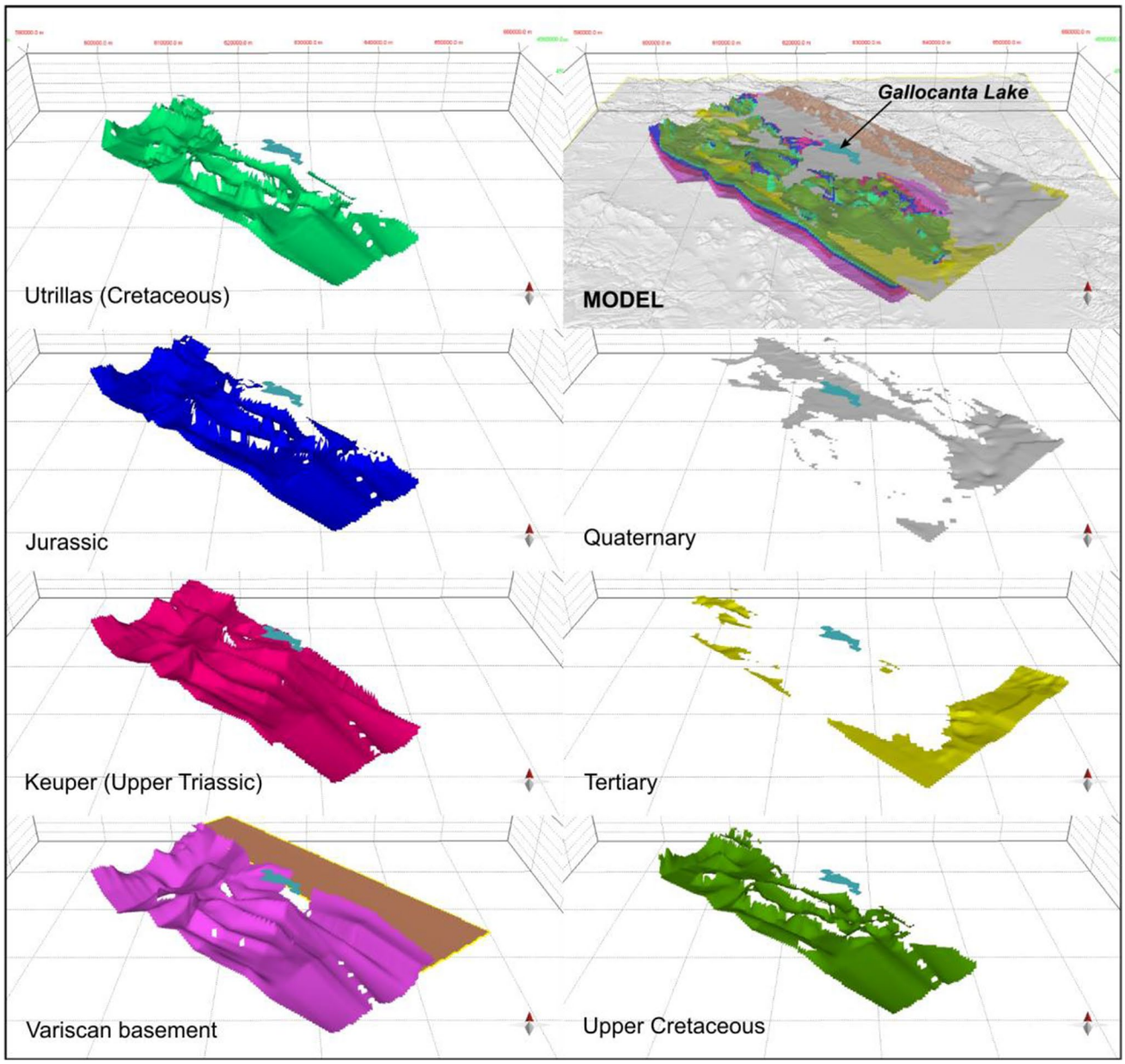

Fig. 5 Hydrogeological units in the 3D geological model

Gallocanta Lake. All these features themselves represent an advance regarding the previous geological model.

The resulting geological map also delimits outcrops more accurately when compared to previous works developed by Gracia *et al.* (2002) or CHE (2003). In particular, the new map includes some of the small Triassic outcrops (Buntsandstein and Muschelkalk facies) at the surroundings of the Gallocanta Lake. It also reviews the extension and thickness of the Keuper outcrops in detail to avoid overestimations or an inadequate extension. Finally, special attention was also paid to Mesozoic materials due to their essential role in the groundwater system of the basin. The characteristics of the Cretaceous outcrops across the western part of the study area were precisely defined, and the interaction and direction of the Jurassic materials, both at the north and south limits of the model, were analysed.

Additionally, 3D geology software allows reaching greater accuracy in terms of the definition and extension of the proposed horizons (bottom and top of the hydrogeological units). The extension of the basal surface of the Jurassic unit, which is the basis of the groundwater system, has been determined with greater accuracy. The morphology of this unit will determine both the main flow directions and groundwater input to Gallocanta Lake. The tectonics and

the distribution of the impermeable Keuper materials at the bottom of the aquifer control its geometry.

Implication of the new geological model

Updating the previous 2D model to the 3D model created in this work provides a more detailed conceptual understanding of the geology of the Gallocanta Basin. The development of a 3D geological model by precisely defining the position of the limits of the hydrogeological units allows establishing the geometry of the bottom of the aquifer to determine the discharge points or flow lines. In addition, it is possible to determine the real recharge area of each hydrogeological unit. It also lets us estimate the groundwater transfers between the Gallocanta Basin and the adjacent basins (Piedra-Ortiz Basin and Jiloca Basin). Not in vain, the presence and relevance of interbasin groundwater flow among adjoining groundwater bodies, of groundwater divides, and the influence of geological structures on groundwater flow dynamics is being tested. Interbasin groundwater flow is an important factor to be considered in the water balance of watersheds. Thus, the geological model presented in this work was implemented as the geological settings in a new hydrogeological model.

Therefore, based on the geological model, it has been possible to develop a robust hydrogeological model that allowed to delve into some of the main uncertainties of the hydrogeological system of Gallocanta. Some of those uncertainties, related to the groundwater transfer to the Jiloca River from the Cretaceous aquifers, are now conveyed through the discharge of the Caminreal Springs (*Ojos de Caminreal)*. These springs would be the preferential discharge area of the Gallocanta basin, which include the Jurassic materials and partially those of the Cretaceous. The flow is determined by the presence and outcrops of impermeable Triassic materials, and it is affected by the existence of Keuper rocks. In addition, in the northwest part of the model, there is an area in which the flow direction can vary based on the head level due to the geological structure. Groundwater flows from Jurassic and Cretaceous units would be towards the Piedra River (North), and only when head level is high enough, water would be partially directed towards the Gallocanta Lake.

Conclusions

The present research has allowed us to delimit the geology of the Gallocanta Basin and the geological structure of the multilayer aquifer that feeds the Gallocanta Lake. The new three-dimensional model has been the basis for developing a hydrogeological model of the area.

The accuracy of the three-dimensional geological model has also proven the effectiveness of three-dimensional software as a suitable and useful tool for geological reconstruction of an area with a complex geological structure such as the Iberian Range. The modelling of the Keuper diapirs, the Triassic rocks and the delimitation of geological units, faults and folds are solved more precisely and realistic using 3D software when compared to previous models and geological maps.

In this way, the model allows establishing the hydrogeological boundaries of the study area and the height of the bottom of each geological unit, which is essential for determining the preferential groundwater flow directions. The accuracy when calculating the height of those bottoms also allows estimating the location of wells and natural springs. The new geological model highlights two potential hydrogeological connections: at the north-western part of the study area, groundwater would flow towards the Piedra River on a seasonal basis; and, at the south part of the study area, groundwater would flow towards the Jiloca River and water springs at Caminreal Springs. This potential hydrogeological connection needs to be studied further, so it is being already explored through a specific hydrogeological model of the Gallocanta Basin.

Author contributions All authors contributed to the study conception and design. Material preparation, data collection and analysis were performed by Javier Ramajo, Carlos Galé and José María Orellana-Macías. The first draft of the manuscript was written by Javier Ramajo and José María Orellana-Macías and all authors commented on previous versions of the manuscript. All authors read and approved the final manuscript.Availability of Data and MaterialsJosé María Orellana-Macías should be contacted if someone wants to request the data.

Funding This work was supported by the Government of Aragon under grant C137/2016; and the Spanish Ministry of Economy and Competitiveness – FEDER funds [EU] via the Research Project Agro-SOS under grant PID2019-108057RB-I00.

Gobierno de Aragón,C137/2016,Ministerio de Ciencia e Innovación,PID2019-108057RB-I00

Data availability Please contact authors for data requests.

All authors contributed to the study conception and design. Material preparation, data collection and analysis were performed by Javier Ramajo, Carlos Galé and José María Orellana-Macías. The first draft of the manuscript was written by Javier Ramajo and José María Orellana-Macías and all authors commented on previous versions of the manuscript. All authors read and approved the final manuscript.

Declarations

Competing interests The authors declare no competing interests.

Conflicts of interest The authors declare no conflict of interest.

References

Aguilar MJ, Ramírez del Pozo J, Riba O (1971) Algunas precisiones sobre la sedimentación y paleoecología del Cretácico inferior en la zona de Utrillas-Villarroya de los Pinares (Teruel). Estudios Geológicos 27:497–512

Alvaro M, Capote R, Vegas R (1979) Modelo de evolución geotectónica para. Acta Geològica Hispànica 14:172–177

Arthaud F, Matte P (1975) Les decrochements tardi-hercyniens du sud-ouest de l'europe. Geometrie et essai de reconstitution des conditions de la deformation. *Tectonophysics, 25*(1–2). https://doi.org/10.1016/0040-1951(75)90014-1

Artimo A, Mäkinen J, Berg RC, Abert CC, Salonen VP (2003) Three-dimensional geologic modeling and visualization of the Virttaankangas aquifer, southwestern Finland. Hydrogeology Journal 11(3):378–386. https://doi.org/10.1007/s10040-003-0256-6

Bascones L, Martín D (1979) Mapa Geológico de España, E.1:50.000 nº 515 (El Pobo de Dueñas). Segunda serie (MAGNA). IGME

Bauluz B, Fernandez-Nieto C, Gonzalez Lopez JM (1998) Diagenesis-very low-grade metamorphism of clastic Cambrian and Ordovician sedimentary rocks in the Iberian Range (Spain). Clay Minerals 33(3):373–393. https://doi.org/10.1180/000985598545697

Ballesteros D, Malard A, Jeannin PY, Jiménez-Sánchez M, García-Sansegundo J, Meléndez-Asensio M, Sendra G (2015) KARSYS hydrogeological 3D modeling of alpine karst aquifers developed in geologically complex areas: Picos de Europa National Park (Spain). Environmental Earth Sciences 74(12):7699–7714. https://doi.org/10.1007/s12665-015-4712-0

Berg RC, Thorleifson H (2001) Geological Models for Groundwater Flow Modeling. En *35th Annual Meeting. North-Central Section. Geological Sociery of America* (p. 72). Normal: Illinois State Geological Survey

Béthoux N, Theunissen T, Beslier MO, Font Y, Thouvenot F, Dessa JX, …, Guillen A (2016) Earthquake relocation using a 3D a-priori geological velocity model from the western Alps to Corsica: Implication for seismic hazard. Tectonophysics 670:82–100. https://doi.org/10.1016/j.tecto.2015.12.016

Burjachs F, Rodó X, Comín F (1996) Gallocanta: Ejemplo de secuencia Palinológica en una laguna efímera. En B. Ruiz Zapata (Ed.), *Estudios Palinológicos. XI Simposio de Palinología* (pp. 25–29). Alcalá de Henares: Universidad de Alcalá de Henares

Capote R, Muñoz JA, Simón JL, Liesa CL, Arlegui LE (2002) Alpine tectonics I: the Alpine system north of the betic cordillera. In: Gibbons W, Moreno T (eds) The Geology of Spain. The Geological Society, London, pp 367–400

Carls P (1983) La zona Asturoccidental-Leonesa en Aragón y el Macizo del Ebro como prolongación del Macizo Cantábrico. In IGME (Ed.), Libro Jubilar J.M. Ríos (pp. 11–32). Madrid

Castañeda C, Javier Gracia F, Luna E, Rodríguez-Ochoa R (2015) Edaphic and geomorphic evidences of water level fluctuations in Gallocanta Lake, NE Spain. Geoderma 239–240:265–279. https://doi.org/10.1016/j.geoderma.2014.11.005

CHE (2003) Establecimiento de las normas de explotación de la Unidad Hidrogeológica "Gallocanta" y delimitación de los perímetros de protección de la laguna. Zaragoza

Dantín J (1941) La laguna salada de Gallocanta (Zaragoza). Estudios Geográficos 3:269–303

De Vicente G (2004) Estructura alpina del Antepaís Ibérico. In A. Vera, J (Ed.), Geología de España (pp. 587–634). Madrid: SGE-IGME

Del Olmo P, Portero JM (1980) Mapa geológico de la hoja nº 464 (Used). Mapa Geológico de España E. 1:50.000. Segunda serie (MAGNA), Primera edición. IGME

García A, Segura M, Calonge A, Carenas B (1989) Unidades estratigráficas para la organización de la sucesión sedimentaria del Aptiense- Cenomaniense de la Cordillera Ibérica. In: Vera JA (ed) División de unidades estratigráficas en el análisis de cuencas, vol 2. Revista de la Sociedad Geológica de España, Madrid, pp 303–333

Goy A, Gómez J, Yebenes A (1976) El jurásico de la Rama Castellana de la Cordillera Ibérica (Mitad Norte) I: Unidades litoestratigráficas. Estudios Geológicos 32:391–423

Gracia FJ (1990a) Dinámica Litoral en la Laguna de Gallocanta (Cordilla Ibérica Central). In *I Reunión Nacional de Geomorfología* (pp. 267–276). Teruel: Sociedad Española de Geomorfología

Gracia FJ (1990b) Evolución geomorfológica reciente de la Laguna de Gallocanta (Cordillera Ibérica Central). In *I Reunión Nacional de Geomorfología* (pp. 277–289). Teruel: Sociedad Española de Geomorfología

Gracia FJ (1992) Papel de la karstificación en la evolución cuaternaria de la Laguna de Gallocanta (provincia de Zaragoza). In *Actas del III Congreso Geológico de España* (pp. 58–62). Salamanca: Sociedad Geológica Española

Gracia FJ (1995) Shoreline forms and deposits in Gallocanta Lake (NE Spain). Geomorphology 11:323–335. https://doi.org/10.1016/0169-555X(94)00080-B

Gracia FJ, Gutiérrez F, Gutiérrez M (1999) Evolución geomorfológica del polje de Gallocanta (Cordillera Ibérica). Revista de La Sociedad Geológica de España

Guglielmetti L, Comina C, Abdelfettah Y, Schill E, Mandrone G (2013) Integration of 3D geological modeling and gravity surveys for geothermal prospection in an Alpine region. Tectonophysics 608(November):1025–1036. https://doi.org/10.1016/j.tecto.2013.07.012

Guimerà J (2018) Structure of an intraplate fold-and-thrust belt: The Iberian chain. A synthesis. Geologica Acta 16(4):427–438. https://doi.org/10.1344/GeologicaActa2018.16.4.6

Haldar SK (2018) Exploration Modeling. In S. K. B. T.-M. E. (Second E. Haldar (Ed.), *Mineral Exploration (Principles and Applications)* (pp. 195–209). Elsevier. https://doi.org/10.1016/B978-0-12-814022-2.00010-1

Hassen I, Gibson H, Hamzaoui-Azaza F, Negro F, Rachid K, Bouhlila R (2016) 3D geological modeling of the Kasserine Aquifer System, Central Tunisia: New insights into aquifer-geometry and interconnections for a better assessment of groundwater resources. Journal of Hydrology 539:223–236. https://doi.org/10.1016/j.jhydrol.2016.05.034

Hernández F, Aranegui P (1926) La laguna de Gallocanta y la geología de sus alrededores. Boletín de La Real Sociedad Española de Historia Natural 26:419–429

Hernández A, Olivé A, Moissenet E, Carls P, Sdzuy K, Kolb S (1980a) Mapa geológico de la hoja nº 465 (Daroca). Mapa Geológico de España E. 1:50.000. Segunda serie (MAGNA), Primera edición. IGME

Hernández A, Olivé A, Pardo G, Villena J, Moissenet E (1980b) Mapa geológico de la hoja nº 491 (Calamocha). Mapa Geológico de España E. 1:50.000. Segunda serie (MAGNA), Primera edición. IGME

Howahr M (2016) Water Board of Oldenburg and East Frisia (OOWV) - 3D Geological Models - Application in water resource management and groundwater protection. In *3rd European 3D Geological Modelling meeting* (pp. 1–28). Wiesbaden

Jørgensen F, Høyer AS, Sandersen PBE, He X, Foged N (2015) Combining 3D geological modelling techniques to address variations in geology, data type and density - An example from Southern Denmark. Computers and Geosciences 81:53–63. https://doi.org/10.1016/j.cageo.2015.04.010

Kessler H, Mathers S, Lelliott M, Hughes A, Macdonald D (2007) Rigorous 3D geological models as the basis for groundwater modelling. En H. Thorleifson, R. C. Berg, & H. A. J. Russell (Eds.), *Three-dimensional geologic mapping for groundwater applications. Workshop extended abstracts* (pp. 27–32). Denver: Minnesota Geological Survey

Liesa CL, Casas AM, Simón JL (2018) La tectónica de inversión en una región intraplaca: la Cordillera Ibérica. Revista de la Sociedad Geológica de España 31(2):23–50

López Olmedo et al. 2021 Cartografía Continua Geológica de la Cordillera Ibérica (Z1700) a escala 1:50000 GEODE

Lotze F (1929) Stratigraphie un Tektonik des Keltiberischen Grundgebirges (Spanien). Abhandlungen Der Gesellschaft Der Wissenschaften in Göttingen. Mathematisch-Physikalische Klasse, 14(2), 1–320

Luzón A, Pérez A, Mayayo MJ, Soria AR, Sánchez Goñi MF, Roc AC (2007) Holocene environmental changes in the Gallocanta lacustrine basin, Iberian Range. NE Spain. Holocene 17(5):649–663. https://doi.org/10.1177/0959683607078994

Luzón A, Pérez A, Roc AC, Soria AR, Mayayo MJ, Sánchez J (1999) Subambientes sedimentarios del sector noroeste de Gallocanta, Provincia de Zaragoza. Geogaceta 26:55–58

Malard A, Jeannin PY, Vouillamoz J, Weber E (2015) Approche intégrée pour la délimitation des bassins d'alimentation et la modélisation du réseau de conduits des systèmes karstiques: application au jura tabulaire Suisse. Hydrogeology Journal 23(7):1341–1357. https://doi.org/10.1007/s10040-015-1287-5

Mayayo MJ, Luzón A, Soria AR, Roc AC, Sánchez J, Pérez A (2003) Sedimentological evolution of Holocene Gallocanta Lake, NE Spain. In: Valero B (ed) Limnogeology in Spain: a tribute to Kerry Kelts. Departamento de Publicaciones del CSIC, Madrid, pp 359–384

Mont Terri Project (2017) 3D geological model. https://www.mont-terri.ch/en/geology%20/3D-geological-model.html

Olivé A, Moissenet E, Hernández Samaniego A, Pardo G, Villena J (1980) Mapa Geológico de España, E.1:50.000 nº 516 (Monreal del Campo). Segunda serie (MAGNA). IGME

Pérez-Estaún A, Bea F, Bastida F, Marcos A, Martínez Catalán JR, Martínez Poyatos D, …, Azor A (2004) Macizo Ibérico. In J. A. Vera (Ed.), *Geología de España* (pp. 21–25). Madrid: SGE-IGME

Pérez A, Luzón A, Roc AC, Soria AR, Mayayo MJ, Sánchez JA (2002) Sedimentary facies distribution and genesis of a recent carbonate-rich saline lake: Gallocanta Lake, Iberian Chain. NE Spain. Sedimentary Geology 148(1–2):185–202. https://doi.org/10.1016/S0037-0738(01)00217-2

Pérez A, Roc AC, Luzón A, Soria AR, Mayayo MJ, Sánchez J (1999) Cartography and interpretation of facies from the recent saline lake of Gallocanta, Iberian Range, NE Spain. In *Abstracts 19th IAS Regional European Meeting of Sedimentology* (p. 197). Copenhagen: IAS

PETEX (2017). https://www.petex.com/products/move-suite/

Portero JM, Del Olmo P, Pardo G, Villena J (1980) Mapa Geológico de España, E.1:50.000 nº 490 (Odón). Segunda serie (MAGNA). IGME

Ramos A (1979) *Estratigrafía y paleografía del pérmico y triásico al oeste de Molina de Aragón (Prov. de Guadalajara)*. Universidad Complutense de Madrid

Robins NS, Rutter HK, Dumpleton S, Peach DW (2005) The role of 3D visualisation as an analytical tool preparatory to numerical modelling. Journal of Hydrology 301(1):287–295. https://doi.org/10.1016/j.jhydrol.2004.05.004

Ross M, Parent M, Lefebvre R (2005) 3D geologic framework models for regional hydrogeology and land-use management: A case study from a Quaternary basin of southwestern Quebec. Canada. Hydrogeology Journal 13(5–6):690–707. https://doi.org/10.1007/s10040-004-0365-x

Schütt B (1998) Reconstruction of Holocene paleoenvironments in the endorheic basin of Laguna de Gallocanta, Central Spain by investigation of mineralogical and geochemical characters from lacustrine sediments. Journal of Paleolimnology 20(3):217–234. https://doi.org/10.1023/A:1007924000636

Schütt B (2000) Holocene paleohydrology of playa lakes in northern and central Spain: a reconstruction based on the mineral composition of lacustrine sediments. Quaternary International 73(74):7–27. https://doi.org/10.1016/S1040-6182(00)00062-8

Thornton JM, Mariethoz G, Brunner P (2018) Erratum: Publisher Correction: A 3D geological model of a structurally complex Alpine region as a basis for interdisciplinary research (Scientific data (2018) 5 (180238)). Scientific Data 6(1):325. https://doi.org/10.1038/s41597-019-0298-9

Turk J, Malard A, Jeannin PY, Petrič M, Gabrovšek F, Ravbar N, …, Sordet V (2015) Hydrogeological characterization of groundwater storage and drainage in an alpine karst aquifer (the Kanin massif, Julian Alps). Hydrological Processes, 29(8), 1986–1998. https://doi.org/10.1002/hyp.10313

Turner AK, Gable CW (2007) A review of geological modeling. In Thorleifson H, Berg RC, Russell HAJ (Eds.), *Three-dimensional geologic mapping for groundwater applications. Workshop extended abstracts* (pp. 81–85). Denver: Minnesota Geological Survey

Vanneschi C, Salvini R, Massa G, Riccucci S, Borsani A (2014) Geological 3D modeling for excavation activity in an underground marble quarry in the Apuan Alps (Italy). Computers and Geosciences 69:41–54. https://doi.org/10.1016/j.cageo.2014.04.009

Vilas L, Más JR, García A, Arias C, Alonso A, Melendez N, Rincón R (1982) Ibérica Suroccidental. In: García A (ed) El Cretácico de España. Universidad Complutense de Madrid, Madrid, pp 457–514

Villena J (1969) Mapa geológico de la Laguna de Gallocanta (Teruel-Zaragoza) y sus alrededores. In *V Reunión grupo Esp. Sedimentología*. Pamplona

Virgili C, Sopeña A, Ramos A, Hernando S (1977) Problemas de la cronoestratigrafía del Trías en España. Cuadernos Geología Ibérica 4:57–88

Wellmann F, Schaaf A, de la Varga M, von Hagke C (2019) From Google Earth to 3D Geology Problem 2: Seeing Below the Surface of the Digital Earth. In A. Billi & Å. B. T.-D. en S. G. y T. Fagereng (Eds.), *Problems and Solutions in Structural Geology and Tectonics* (Vol. 5, pp. 189–204). Elsevier. https://doi.org/10.1016/B978-0-12-814048-2.00015-6

Zhu Z, Lei X, Xu N, Shao D, Jiang X, Wu X (2020) Integration of 3D geological modeling and geothermal field analysis for the evaluation of geothermal reserves in the Northwest of Beijing Plain, China. Water (Switzerland), 12(3). https://doi.org/10.3390/w12030638

Zhuang H (2013) Dynamic Well Testing in Petroleum Exploration and Development (Second Edi). Elsevier, Waltham